



HAL
open science

Large Extracellular Cord Formation in a Zebrafish Model of *Mycobacterium kansasii* Infection

Johansen Matt, Kremer Laurent

► **To cite this version:**

Johansen Matt, Kremer Laurent. Large Extracellular Cord Formation in a Zebrafish Model of *Mycobacterium kansasii* Infection. *Journal of Infectious Diseases*, 2020, pp.jiaa187. 10.1093/infdis/jiaa187 . inserm-02868836

HAL Id: inserm-02868836

<https://inserm.hal.science/inserm-02868836>

Submitted on 15 Jun 2020

HAL is a multi-disciplinary open access archive for the deposit and dissemination of scientific research documents, whether they are published or not. The documents may come from teaching and research institutions in France or abroad, or from public or private research centers.

L'archive ouverte pluridisciplinaire **HAL**, est destinée au dépôt et à la diffusion de documents scientifiques de niveau recherche, publiés ou non, émanant des établissements d'enseignement et de recherche français ou étrangers, des laboratoires publics ou privés.

17 **Abstract (100 words)**

18

19 *Mycobacterium kansasii* is a slow-growing non-tuberculous mycobacteria responsible for co-
20 infections particularly in patients with human immunodeficiency virus. To date, our knowledge
21 of *M. kansasii* infection has been hampered due to the lack of an effective animal model to
22 study pathogenesis. Here, we show the zebrafish embryo is permissive to *M. kansasii* infection,
23 causing a chronic infection and forming granulomas. Upon macrophage depletion, we
24 identified *M. kansasii* forms extracellular cords, resulting in acute infection and rapid larval
25 death. These findings highlight the feasibility of zebrafish to study *M. kansasii* pathogenesis,
26 and for the first time identify extracellular cords in this species.

27

28 **Keywords:** *Mycobacterium kansasii*, granuloma, infection, cords, zebrafish, macrophage

29

30

31

32

33

34

35

36

37

38

39 **Background (2000 words)**

40 *Mycobacterium kansasii* is a slow-growing photochromogenic non-tuberculous mycobacteria
41 (NTM). This opportunistic pathogen is a common source of severe pulmonary infections in
42 patients with human immunodeficiency virus (HIV), chronic obstructive pulmonary disorder
43 and generalised immunosuppression [1-3]. It is regarded as one of the phylogenetically closest
44 species to *Mycobacterium tuberculosis* and is clinically indistinguishable based on clinical
45 symptoms and radiographic features [2]. Previous research has reported >50% mortality rates
46 in patients with HIV and *M. kansasii* co-infections [1], representing a significant public health
47 burden in at-risk populations.

48 Despite the significance of *M. kansasii* infections in specific patient subpopulations,
49 there has been very little research exploring pathogenicity of this species. Previous reports
50 demonstrated that type I *M. kansasii* ATCC 12478 is able to rupture the phagosomal membrane
51 similarly to *M. tuberculosis* [4], yet it is only able to cause a persistent non-replicating infection
52 in a murine model [2]. As such, there is an urgent need to explore alternative animal models to
53 study *M. kansasii* pathogenesis. In recent years, the zebrafish has emerged as an important
54 infection model to investigate mycobacterial infections, recapitulating important aspects of the
55 human mycobacterial infection, such as granuloma formation [5-7]. Advancements in genetics
56 have allowed the generation of fluorescently labelled cellular subsets and zebrafish knockout
57 lineages, allowing us to explore specific determinants of host immunity [8]. In particular, the
58 zebrafish embryo is optically transparent and possesses a functional innate immune response
59 from approximately 30 hours post-fertilisation, allowing the visualisation of early host-
60 pathogen interactions at the cellular level [7, 8]. Therefore, we explored whether zebrafish
61 embryos could be used as a model for *M. kansasii* infection and examined initial host-pathogen
62 interactions.

63 **Methods**

64 **Bacterial culture and generation of fluorescent *M. kansasii***

65 *M. kansasii* ATCC 12478 and *M. marinum* M strain (ATCC BAA-535) were grown in
66 Middlebrook 7H9 broth (BD Difco) and supplemented with 0.025% Tyloxapol and 10% oleic
67 acid, albumin, dextrose, catalase (OADC enrichment) (7H9^{OADC/T}) or on Middlebrook 7H10
68 agar (BD Difco) containing 10% OADC enrichment (7H10^{OADC}). Bacteria were cultured at
69 37°C unless otherwise indicated. Antibiotics were included where required for fluorescent
70 strains.

71 Fluorescent *M. kansasii* was generated using pTEC15 and pTEC27 (a gift from Lalita
72 Ramakrishnan) as previously described [9], however 7H9^{OADC/T} was used instead of Sauton's
73 and all incubation and wash steps were completed at 37°C and not 4°C. For selection of
74 fluorescent colonies, *M. kansasii* was plated on 7H10^{OADC} containing 50 µg/mL hygromycin
75 (Euromedex). Positive colonies were selected based on fluorescence and maintained in
76 7H9^{OADC/T} supplemented with 50 µg/mL hygromycin. Fluorescent *M. marinum* M strain has
77 been previously described [10].

78

79 **Zebrafish maintenance and infection**

80 Zebrafish experiments were completed in accordance with the Comité d'Ethique pour
81 l'Expérimentation Animale de la Région Languedoc Roussillon under the reference
82 CEEALR36-1145. Experiments were performed using the *golden* mutant and macrophage
83 reporter Tg(*mpeg1:mCherry*) line, as previously described [6]. Single cell bacterial
84 preparations were completed as previously described [6] and used immediately and not from
85 frozen stocks. Zebrafish caudal vein injections and lipoclodronate macrophage depletion were
86 conducted, as reported [6]. Following infection, embryo age is expressed as days post-infection

87 (dpi). Embryo survival was monitored daily based on the presence of a heartbeat. For live
88 imaging, zebrafish embryos were anaesthetised in 0.02% tricaine solution [6, 10], mounted on
89 3% (w/v) methylcellulose and imaged using a Zeiss Axio Zoom.V16 coupled with an Axiocam
90 503 mono (Zeiss). Fluorescence Pixel Count (FPC) measurements were determined using the
91 ‘Analyse particles’ function in ImageJ and normalised for each experiment against the
92 corresponding control. All experiments were completed at least three times independently.

93

94 **Statistical analysis**

95 Survival curve analysis was completed using the log-rank (Mantel-Cox) statistical test. Cord,
96 granuloma and bacterial burden (FPC) analysis were completed using unpaired Student’s *t*-
97 test. All statistical tests were completed using Graphpad Prism (Version 8.0.1).

98

99 **Results**

100 ***Mycobacterium kansasii* infection causes a chronic infection in zebrafish embryos**

101 A critical characteristic of zebrafish manipulation is the requirement for lower ambient
102 temperatures of 28.5°C. As such, we first determined whether *M. kansasii* can replicate at lower
103 temperatures compared to traditional 37°C incubation. We found that *M. kansasii* is able to
104 grow and replicate at 30°C, albeit slower than at 37°C which was to be expected as for other
105 NTM species [6] (**Supplementary Figure 1**).

106 Previous research has demonstrated that the zebrafish embryo is an attractive model
107 organism for mycobacterial pathogens such as *M. marinum* and *M. abscessus* and
108 recapitulating important pathophysiological hallmarks of human mycobacterial infection and
109 leading to larval death [6, 7]. With this in mind, we wanted to determine whether *M. kansasii*
110 was able to promote larval death in a dose-dependent manner. We found that *M. kansasii*

111 resulted in $\leq 10\%$ embryo mortality in a 12-day period, irrespective of infectious dose.
112 Comparatively, *M. marinum*, which is an important fish and human pathogen, led to 100%
113 embryo mortality within 9 dpi (**Figure 1A**), as previously reported [7].

114 We next wanted to explore whether *M. kansasii* ATCC 12478 is rapidly cleared
115 following infection, or whether it causes a persistent infection. Using live whole embryo
116 fluorescent imaging, we observed the formation of granulomas in 50-60% of embryos from 3
117 dpi onwards (**Figure 1B-D**). Moreover, when we examined the average number of granulomas
118 per infected embryo over time, we observed a trend for the increasing number of granulomas
119 between 3 and 9 dpi, however this was not significant ($P = 0.06$) (**Supplementary figure 2**).
120 Overall, these results highlight that the zebrafish embryo is permissive to *M. kansasii* infection,
121 leading to a chronic infection characterised by granuloma formation.

122

123 ***Mycobacterium kansasii* is able to form large extracellular cords and resist phagocytosis**

124 Macrophages are important immune cells recruited to an infection and are the predominant cell
125 subset within the mycobacterial granuloma [7, 11]. Previous work showed that macrophage
126 ablation results in rapid larval death within several days of infection, underpinning the crucial
127 role of these phagocytes in containing mycobacterial infections [6, 12]. Thus, we explored
128 whether macrophages are responsible for *M. kansasii* infection control. Following liposomal
129 clodronate treatment, which depletes macrophages until approximately 6 days post-treatment
130 (**Supplementary figure 3**), we observed progressive larval death resulting in ~70% of dead
131 embryos at 12 dpi as compared to standard *M. kansasii* infection or following liposomal PBS
132 injection prior to infection (**Figure 2A**). When we examined the bacterial burden in clodronate-
133 treated embryos, there was a significant increase from 2 dpi onwards when compared to wild-
134 type infections (**Figure 2B**).

135 Using whole embryo live fluorescent imaging in clodronate-treated embryos, we
136 identified the presence of large extracellular cords in 20% of embryos from 3 dpi, which
137 increased to >80% by 9 dpi (**Figure 2C**). Comparatively, extracellular cord formation in wild-
138 type embryos was a rare event, occurring in <10% of infected embryos and only at 9 dpi
139 (**Figure 2C**). When we further categorised the proportion of cords per embryo, we identified a
140 progressive increase in the number of moderate (6-10 cord/embryo) and heavy (>10
141 cords/embryo) number of cords up to 9 dpi, as compared to 3 dpi in which 100% of corded
142 embryos had a low number of cords (1-5 cords/embryo) (**Figure 2C**). Following macrophage
143 repopulation at 6 days post clodronate-treatment, we observed the gradual recruitment of
144 macrophages to extracellular cords at approximately 9 dpi (**Figure 2D**). However, based on the
145 sheer size of these observed cords in comparison to the size of the recruited macrophages, they
146 were unable to degrade or control cord formation, in agreement with the increase in the number
147 of embryos with cords and the average number of cords (**Figure 2C**). Finally, to determine if
148 cord formation is an acquired *in vivo* phenotype of *M. kansasii*, we examined stationary-phase
149 liquid cultures for the presence of cords. Using fluorescent microscopy, we observed the
150 presence of large bacterial aggregates resembling cords, demonstrating that this is an intrinsic
151 *M. kansasii* phenotype (**Supplementary Figure 4**).

152 Collectively, these findings highlight the critical role of macrophages in the control of
153 *M. kansasii* infection and preventing the formation of large extracellular cords. Importantly, to
154 our knowledge this is the first reported observation of *M. kansasii* cord formation both *in vitro*
155 and *in vivo*, which has significant implications for our understanding of *M. kansasii*
156 pathogenesis.

157

158

159

160 Discussion

161 In this study, we report for the first time the applicability of the zebrafish embryo to study the
162 pathogenesis of *M. kansasii*. Using this model organism, we demonstrate that under standard
163 infection conditions, a type I *M. kansasii* strain causes a persistent and replicating infection
164 typified by the presence of mycobacterial granulomas. Most importantly, we report here that
165 *M. kansasii* forms large extracellular cords, representing a significant pathogenic trait of this
166 NTM that was previously unexplored.

167 In recent years, the zebrafish model has established itself as a revolutionary platform to
168 examine host-pathogen interactions in real-time [7, 8]. Using this to our advantage in the
169 current study, we were able to monitor the kinetics of granuloma formation following *M.*
170 *kansasii* infection which revealed a chronic *in vivo* phenotype, representative of other slow-
171 growing mycobacteria, including *M. tuberculosis*. It is notable that the zebrafish embryo does
172 not possess adaptive immunity until later developmental stages and as such, the role of adaptive
173 immunity in *M. kansasii* remains unexplored. However, adult zebrafish have fully functional
174 innate and adaptive immunity and may be a feasible model organism to examine the role of
175 complete immunity of *M. kansasii* infection in subsequent studies.

176 Cord formation is a pathophysiological hallmark of acute mycobacterial disease [6, 13-
177 15]. Following the successful escape from the phagosome, mycobacteria such as *M. abscessus*,
178 *M. marinum* and *M. tuberculosis* [4], are able to grow extracellularly as large cords which
179 vastly exceed the size of recruited immune cells and ultimately resist phagocytosis [6]. To date,
180 this phenotypic characteristic has only been identified within a few pathogenic mycobacteria
181 species and has often been reserved for those that have been considered most virulent. We
182 report here, the formation of large extracellular cords in *M. kansasii* both *in vitro* and *in vivo*.
183 That *M. kansasii* shares this phenotypic trait with *M. tuberculosis* further supports the recent

184 view that *M. kansasii* is an environmental ancestor of *M. tuberculosis* and can be used as a
185 model organism to investigate the transition from an environmental opportunistic pathogen to
186 a host-restricted pathogen [2]. Following macrophage depletion, we observed a large increase
187 in the presence and abundance of cords, highlighting the importance of macrophages in *M.*
188 *kansasii* infection. Severe infections with *M. kansasii* are often associated with co-existing
189 infections such as HIV, suggesting that immunodeficiency is an important risk factor in the
190 severity of *M. kansasii* infection [3]. Consequently, our observations of extensive cord
191 formation following macrophage ablation may be viewed as clinically relevant and may
192 provide an explanation for the higher mortality rate associated with *M. kansasii* co-infection in
193 immunocompromised patients. As this is the first report of cord formation in *M. kansasii*, it is
194 important that subsequent studies examine the role of cord formation in clinical isolates and
195 screen patient sputum for the presence of *M. kansasii* extracellular cords to support these
196 observations.

197 While cording in wild-type embryos can be considered a rare event in the context of the
198 current study, it is not entirely absent suggesting that *M. kansasii* can eventually escape from
199 the phagosome. This observation fits with previous work which has identified that *M. kansasii*
200 is able to rupture the phagosomal membrane, indicative of phagosomal escape [2, 4]. Moreover,
201 *M. kansasii* has been demonstrated to secrete *esxA* and *esxB*; two effector proteins of the well-
202 characterised ESX-1 locus, which are known to assist in phagosomal escape for *M. marinum*
203 and *M. tuberculosis* [2]. However, to date, the role of ESX-1 in *M. kansasii* pathogenesis
204 remains to be explored.

205 In summary, our findings highlight the applicability of the zebrafish embryo to examine
206 host-pathogen interactions and pathogenesis for the study of *M. kansasii*. Furthermore, using
207 our new animal model, we have demonstrated that *M. kansasii* causes a chronic infection which
208 is largely controlled by patrolling macrophages in a wild-type infection. Most importantly, we

209 have shown that *M. kansasii* forms large cords both *in vitro* and *in vivo*, ultimately representing
210 a previously unexplored virulence trait of this clinically significant NTM species.

211

212 **Funding**

213 MDJ received a post-doctoral fellowship granted by Labex EpiGenMed, an «Investissements
214 d’avenir» program (ANR-10-LABX-12-01).

215

216 **Conflicts of interest**

217 The authors have no conflict of interest to declare.

218

219 **Figure legends**

220 **Figure 1: *Mycobacterium kansasii* induces a chronic infection in zebrafish.** (A) Zebrafish
221 embryos at approximately 30 hours post-fertilisation were infected with increasing doses of *M.*
222 *kansasii* ATCC 12478, or 100 CFU of *M. marinum* M strain *via* caudal vein injection and
223 survival was monitored over a 12-day period. Each group consists of approximately 20
224 embryos, with each experiment completed at least three independent times. Statistical
225 significance was determined using the log-rank (Mantel Cox) test. (B) The proportion of
226 infected zebrafish embryos with granulomas detected *via* fluorescent microscopy at 3, 6 and 9
227 days post-infection (dpi). Each experiment was completed three independent times, with
228 approximately 20 embryos per group. Error bars represent standard deviation. Statistical
229 analysis was completed using the Student’s *t*-test. (C) Example image of granulomas located
230 in the trunk region of zebrafish embryos infected with *M. kansasii* at 9 dpi. Macrophages are
231 labelled in red, while *M. kansasii* is labelled in green. Granulomas are highlighted with white
232 arrows. Scale bar represents 1 mm. (D) Representative image of several macrophages (red)

233 infected with *M. kansasii* (green) forming a granulomatous infection foci at 9 dpi. Scale bar
234 represents 100 μm .

235

236 **Figure 2: Macrophages are critical determinants of host immunity to *M. kansasii* infection**

237 **and prevent extracellular cord formation. (A)** Zebrafish embryos at 24 hours post-

238 fertilisation were injected with lipoclodronate *via* caudal vein injection to deplete macrophages.

239 Following 6 hours treatment, embryos were infected with 300 CFU *M. kansasii* ATCC 12478

240 *via* caudal vein injection and survival was monitored daily over a 12-day period. Statistical

241 significance was determined using the log-rank (Mantel Cox) test. **(B)** Bacterial burden was

242 quantified by fluorescent pixel counts (FPC) using ImageJ, with each point representing an

243 individual embryo. Error bars represent standard deviation. Statistical analysis was completed

244 using the Student's *t*-test. **(C)** The proportion of infected zebrafish embryos with extracellular

245 cords detected (left panel) and the average number of cords per embryo split into low (1-5

246 cords/embryo), moderate (6-10 cords/embryo) and high (>10 cords/embryo) number of cords

247 per embryo (right panel) that were detected using fluorescent microscopy at 3, 6 and 9 days

248 post-infection (dpi). The number of embryos analysed is indicated into brackets. Error bars

249 represent standard deviation. Statistical analysis was completed using Student's *t*-test. **(D)**

250 Representative images of extracellular cords identified using whole embryo live fluorescent

251 microscopy on the trunk region at 6 dpi (left panel) and 9 dpi (right panel). Macrophages are

252 labelled in red and *M. kansasii* is labelled in green. Cords are highlighted with white arrows.

253 Scale bars represent 1 mm and 100 μm , respectively. *** $P \leq 0.001$, **** $P \leq 0.0001$. ns, non-

254 significant.

255

256 **Supplementary Figure 1: *M. kansasii* is able to replicate at lower temperatures. *M.***

257 *kansasii* ATCC 12478 was inoculated in 7H9^{OADC/T} at an optical density of 0.05 (OD₆₂₀) and

258 incubated at 30°C and 37°C under shaking at 100 rpm. Growth measurements were taken daily
259 over a 16-day period until cultures reached stationary phase.

260

261 **Supplementary Figure 2: Average numbers of granulomas per embryo over time.**

262 Macrophage reporter embryos Tg(*mpeg1:mCherry*) at approximately 30 hours post-
263 fertilisation were infected with 300 CFU of *M. kansasii* ATCC 12478 *via* caudal vein injection.
264 The average number of granulomas per infected zebrafish embryos was detected *via*
265 fluorescent microscopy at 3, 6 and 9 days post-infection (dpi). Each experiment was completed
266 three independent times, with approximately 20 embryos per group. Error bars represent
267 standard deviation. Statistical analysis was completed using the Student's *t*-test.

268

269 **Supplementary figure 3: Efficacy of liposomal clodronate macrophage depletion and
270 restoration kinetics.**

271 Macrophage reporter embryos Tg(*mpeg1:mCherry*) at 24 hours post-
272 fertilisation were injected with either PBS clodronate or liposomal clodronate *via* caudal vein
273 injection to deplete macrophages (in red). Following 6 hours treatment, embryos were infected
274 with 300 CFU *M. kansasii* ATCC 12478 (in green). Embryos were monitored at 3 and 6 dpi to
275 determine the rate of regeneration of macrophages in treated embryos. Scale bars represent
276 1mm.

276

277 **Supplementary Figure 4: *M. kansasii* forms large bacterial cords under standard *in vitro*
278 culture conditions.**

279 *M. kansasii* ATCC 12478 was inoculated in 7H9^{OADC/T} at an optical
280 density of 0.05 (OD₆₂₀) and incubated at 37°C with no agitation for approximately 2 weeks,
281 after which bacteria were mounted onto a glass slide and visualised using fluorescent
282 microscopy. Scale bars presents 50 µm.

282 **References**

- 283 1. Marras TK, Morris A, Gonzalez LC, Daley CL. Mortality prediction in pulmonary
284 *Mycobacterium kansasii* infection and human immunodeficiency virus. *Am J Respir Crit Care*
285 *Med* **2004**; 170:793-8.
- 286
- 287 2. Wang J, McIntosh F, Radomski N, *et al.* Insights on the emergence of *Mycobacterium*
288 *tuberculosis* from the analysis of *Mycobacterium kansasii*. *Genome Biol Evol* **2015**; 7:856-70.
- 289
- 290 3. Lovell JP, Zerbe CS, Olivier KN, *et al.* Mediastinal and disseminated *Mycobacterium*
291 *kansasii* disease in GATA2 deficiency. *Ann Am Thorac Soc* **2016**; 13:2169-73.
- 292
- 293 4. Houben D, Demangel C, van Ingen J, *et al.* ESX-1-mediated translocation to the cytosol
294 controls virulence of mycobacteria. *Cell Microbiol* **2012**; 14:1287-98.
- 295
- 296 5. Madigan CA, Cameron J, Ramakrishnan L. A zebrafish model of *Mycobacterium leprae*
297 granulomatous infection. *J Infect Dis* **2017**; 216:776-9.
- 298
- 299 6. Bernut A, Herrmann J-L, Kissa K, *et al.* *Mycobacterium abscessus* cording prevents
300 phagocytosis and promotes abscess formation. *Proc Nat Acad Sci USA* **2014**; 111:943-52.
- 301
- 302 7. Davis JM, Clay H, Lewis JL, Ghori N, Herbomel P, Ramakrishnan L. Real-time visualization
303 of mycobacterium-macrophage interactions leading to initiation of granuloma formation in
304 zebrafish embryos. *Immunity* **2002**; 17:693-702.
- 305
- 306 8. Cronan MR, Tobin DM. Fit for consumption: zebrafish as a model for tuberculosis. *Dis*
307 *Model Mech* **2014**; 7:777-84.

308

309 9. Viljoen A, Gutierrez AV, Dupont C, Ghigo E, Kremer L. A simple and rapid gene disruption
310 strategy in *Mycobacterium abscessus*: On the design and application of glycopeptidolipid
311 mutants. *Front Cell Infect Microbiol* **2018**; 8:69.

312

313 10. Takaki K, Davis JM, Winglee K, Ramakrishnan L. Evaluation of the pathogenesis and
314 treatment of *Mycobacterium marinum* infection in zebrafish. *Nat Protoc* **2013**; 8:1114-24.

315

316 11. Ramakrishnan L. Revisiting the role of the granuloma in tuberculosis. *Nature Reviews*
317 *Immunology* **2012**; 12:352-66.

318

319 12. Clay H, Davis JM, Beery D, Huttenlocher A, Lyons SE, Ramakrishnan L. Dichotomous
320 role of the macrophage in early *Mycobacterium marinum* infection of the zebrafish. *Cell Host*
321 *Microbe* **2007**; 2:29-39.

322

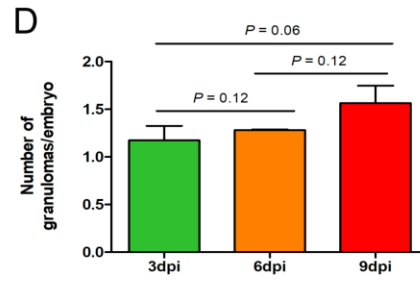
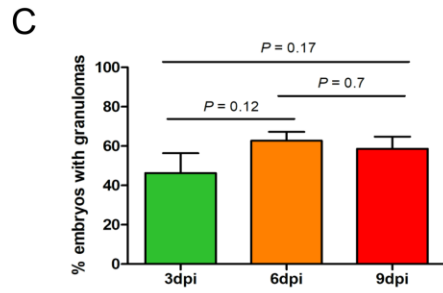
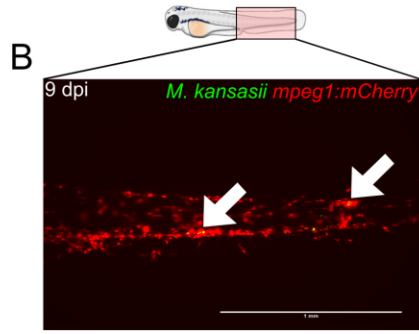
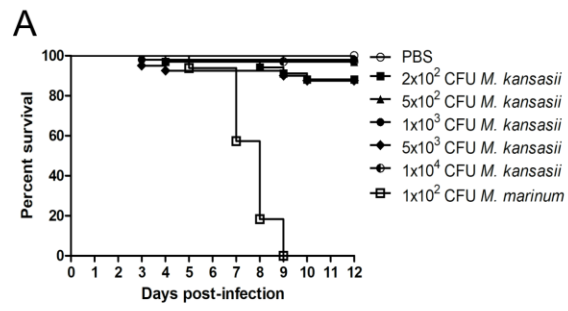
323 13. Julian E, Roldan M, Sanchez-Chardi A, Astola O, Agusti G, Luquin M. Microscopic cords,
324 a virulence-related characteristic of *Mycobacterium tuberculosis*, are also present in
325 nonpathogenic mycobacteria. *J Bacteriol* **2010**; 192:1751-60.

326

327 14. Sanchez-Chardi A, Olivares F, Byrd TF, Julian E, Brambilla C, Luquin M. Demonstration
328 of cord formation by rough *Mycobacterium abscessus* variants: implications for the clinical
329 microbiology laboratory. *J Clin Microbiol* **2011**; 49:2293-5.

330

331 15. Middlebrook G, Dubos RJ, Pierce C. Virulence and morphological characteristics of
332 mammalian tubercle bacilli. *J Exp Med* **1947**; 86:175-84.



334

335

